Int J Adv Manuf Technol (2012) 60:825–839
DOI 10.1007/s00170-011-3588-8

ORIGINAL ARTICLE

Vehicle dynamics analysis of a heavy-duty commercial vehicle by using multibody simulation methods

Selim Hasagasioglu · Koray Kilicaslan · Orhan Atabay · Ahmet Güney

Received: 14 September 2010 / Accepted: 17 June 2011 / Published online: 2 September 2011

Abstract In this paper, the computer-aided vehicle dynamics analysis of a 6×2 heavy-duty commercial vehicle is examined. For the analysis, Mechanical Simulation Corporation's TruckSim multibody dynamics simulation and SuspensionSim multibody statics simulation softwares are used. The aim of this study is to design and model the front suspension and tandem rear axle suspensions, compose the full-vehicle model representing the real-life vehicle, and examine the dynamic behavior of this model. The models related to the front and rear suspensions are prepared and solved in SuspensionSim and the solutions are imported thereafter to TruckSim. The full-vehicle model excluding the suspension system is formed by using TruckSim. The simulation scenarios, runs of which are made to observe the effects of different parameters concerning the dynamic behavior of the full-vehicle model, are also prepared in TruckSim environment.

Keywords Vehicle dynamics · Simulation · Commercial vehicle · SuspensionSim · TruckSim

S. Hasagasioglu (✉) · K. Kilicaslan
Mercedes-Benz Türk Corporation,
Research and Development Center,
Istanbul, Turkey
e-mail: selim.hasagasioglu@daimler.com

S. Hasagasioglu
e-mail: selimhas@gmail.com

K. Kilicaslan
e-mail: koray.kilicaslan@daimler.com

O. Atabay · A. Güney
Automotive Technologies Research and Development Center,
Istanbul Technical University,
Istanbul, Turkey

1 Introduction

Computer-aided modeling and simulation are becoming one of the methods used frequently on research and development (R&D) activities in today's automotive industry. The definitive aim of such activities is to lessen the time and the money spent. In addition, considering the complexity of design process of a vehicle and intense competition in the market, simulation researches are more of importance. The indicator and requirement of today's modernity is implementing and stimulating those tools more and more on R&D activities.

Multibody stimulation is one of the methods that help to constitute a dynamic model of a real mechanical system. An engineer using multibody dynamics programs such as ADAMS does not need to derive and solve the governing equations of the system; thus, the room for error in doing these calculations will be reduced. Nevertheless, engineers using these programs should learn how to develop a model that comprises essential components. According to Sayers, deriving equations of motion manually and fine-tuning simulation systems that are going to solve these equations are proper methodologies for real-time applications [1].

Some numerical multibody programs use explicit methods that have a clear sequence of calculations that rely on current and past values of a state variable itself and its first derivative, while some using implicit methods that involve looking ahead and calculating derivatives at a future time, using iteration to confirm that the calculated values of the state variable and their derivatives are consistent. In general, implicit methods do not work well for real-time hardware-in-the-loop systems. As with variable-step methods, implicit methods also can complicate the merging of equations from different sources. However, implicit methods are required for some classes of equations, such as differential algebraic equations that

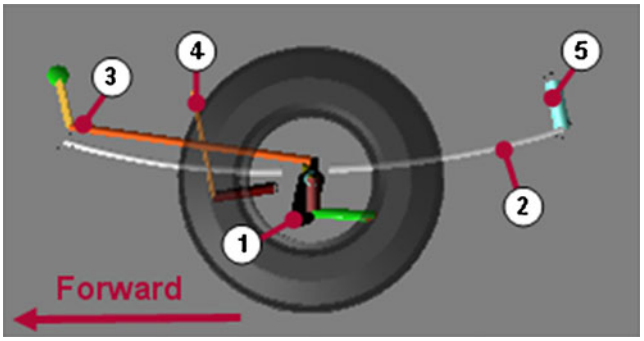

Fig. 1 A schematic drawing of the front suspension

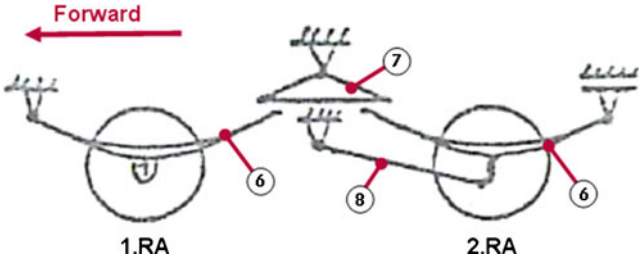

Fig. 3 A schematic drawing of the rear suspension. *1.RA* first rear axle and *2.RA* second rear axle, respectively

are used with some numerical multibody programs such as ADAMS. The equations for vehicle models developed with VehicleSim (VS), the simulation design whose products are CarSim, TruckSim, and BikeSim, are typically well-behaved ordinary differential equations that do not require the extra complexity of implicit solution methods. All integration methods provided in VS solver programs are explicit [2].

Both TruckSim and ADAMS are multibody dynamics programs; however, they differ from each other in some aspects. The difference in modeling methodology is worth mentioning. ADAMS represents the vehicle at component levels, whereas TruckSim represents them at system levels. For example, ADAMS allows the engineer to describe a suspension by the linkage and bushing components of which it is comprised, and thereafter solves for the kinematics and compliances during the course of simulating a total vehicle. On the other hand, TruckSim allows the engineer to describe the suspension by its functional behavior, i.e., by tabular data describing its kinematic and compliance behavior in the three translational and rotational directions [3].

An example of a system simulation of a truck/semitrailer combination is given in [4], where IPG's TruckMaker is used to test electronic chassis control system of the vehicle. TruckMaker offers a library of completely nonlinear truck and trailer models, such as two-, three-, and four-axle trucks; one-, two-, and three-axle semi-trailers as well as two- and three-axle drawbar trailers as is the case in TruckSim. The models in [4] have rigid axles as well as independent wheel suspensions. Axle kinematics and elastokinematics are calculated within TruckMaker environment. State variables such as lateral acceleration and roll angle are calculated through the course of a lane change maneuver, and simulation results are presented accordingly.

In [5], an example of a tractor/trailer vehicle simulation is provided where a TruckSim model and a Simulink model are integrated such that the two models run in parallel. Based on the test data, a Roll Stability Control (RSC) system is developed in Simulink, while the complete vehicle model excluding the RSC system model is developed in TruckSim. Several simulations of a J-turn maneuver and a fishhook maneuver are performed to determine the capability of the RSC system in preventing rollovers under different loading conditions. This study also provides an example of executing highly difficult maneuvers without safety concerns.

There are also examples where ADAMS is used to simulate dynamic behavior of heavy duty vehicles. In [6], ADAMS is used to evaluate ride comfort and stability of a 6 degrees of freedom full-vehicle model of a heavy-duty truck. The model in [6] incorporates all sources of compliance: stiffness and damping with linear and non-linear characteristics, and it also includes the front and rear

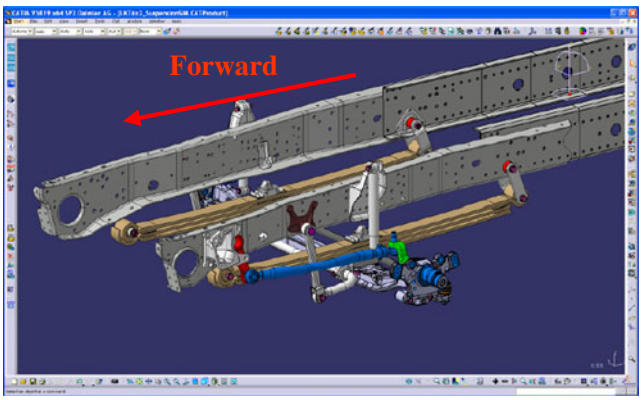

Fig. 2 CATIA 3D model of the front suspension

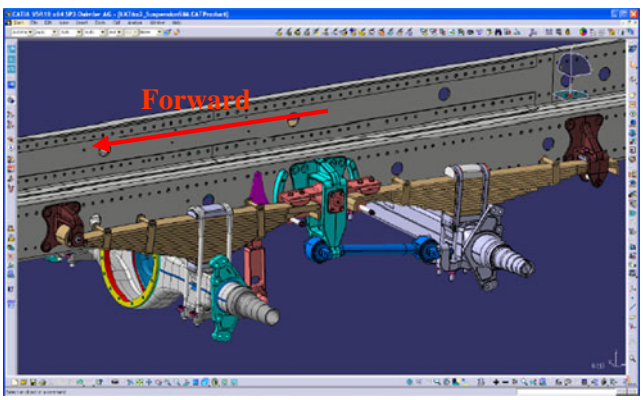

Fig. 4 CATIA 3D model of the rear suspension

Table 1 Components of the front and rear suspension system numbered in Figs. 1 and 3

Number	Component
1	Front axle
2	Leaf springs (front)
3	Steering system
4	Stabilizer bar
5	Shackles
6	Leaf springs (rear)
7	Load equalizer
8	Bar-type radius rods

suspension elements. The road input is excited using four irregular drums, producing the road profile that simulates either smooth flat roads or rough roads with 100-mm bumps. The vehicle model is simulated at different velocities on different road profiles. The results of the analysis provide displacement, acceleration, and pitch angle values of the body on different road profiles as well as front and rear suspension forces through the course of the simulation.

In this paper, the vehicle dynamics analysis of a heavy-duty commercial vehicle launched in 2009 onto market is investigated by using multibody simulation (MBS) methods. The models of the entire suspension system and the full-vehicle model are built using SuspensionSim and TruckSim MBS softwares. The rear suspension system of the vehicle, which is called "four spring suspension with bar type radius rods", is

a

Bodies

Body Name	Letters	Symmetry
Axle	AX	X
Spring at Front Bushing	FE	X
Spring at Shackle	SS	X
Shackle	Sh	X
Knuckle	Kn	X
Pitman Arm	PA	

b

Bodies

Body Name	Letters	Symmetry
Axle and Hub	Ax	X
Spindle - front	Sf	X
Leaf at front Hanger L1	L1	X
Leaf - Frtt Sprg at equal	L4	X
Axle - rear	Ar	X
Lower Link rear	Llr	X
Spindle rear	Sr	X
Load Equalizer	LE	X
Leaf rear at equal L5	L5	X
Leaf rear at rear hanger	L8	X

Fig. 5 The bodies of SuspensionSim models. **a** The bodies for front suspension. **b** The bodies for rear suspension

a

Points

Point Name	Letter	X (mm)	Y (mm)	Z (mm)	Relative
Wheel Center	Wc	.00	977.50	.00	X
Axle Center	Ac	.00	.00	.00	
Kingpin ref (UBJ)	Kr	.00	850.00	.00	X
Tie Rod Outer	To	210.00	803.50	-135.00	
Steer Arm	Sa	.00	659.20	63.40	
Pitman at Drag Link	P1	-873.00	-640.00	221.00	
Pitman Arm at Gear	P2	-916.00	-587.00	403.00	X
Kingpin at Spindle (LBJ)	Kp	.00	868.00	-114.00	X
Kröpfung	K1	-30.00	570.00	-120.00	

b

Points

Point Name	Letter	X (mm)	Y (mm)	Z (mm)	Relative
Wheel Center	Wc	.00	919.00	.00	X
Spindle to Hub	SH	.00	819.00	.00	
Rear Wheel Center	Wr	1,350.00	919.00	.00	X
Lower Link rr at frame	R3	615.00	511.00	155.00	X
Lower Link rr at Axle	R4	1,177.00	511.00	-24.00	X
Spindle at Hub Rear	Sr	1,350.00	819.00	.00	
Front Axle Center	Ac	.00	.00	.00	X
Rear Axle Center	Ac	1,350.00	.00	.00	X
Equalizer Pivot	Pv	617.00	511.00	388.00	
L1 Leaf at front hanger	L1	-746.00	511.00	408.00	X
L4-Leaf frt at frt of equal	L4	458.00	511.00	378.00	X
L5 Leaf rr at rr of equal	L5	829.00	511.00	374.00	X
L8 Leaf rr at rear hanger	L8	2,026.00	511.00	341.00	X
L2 point on frt axle	L2	-76.00	511.00	278.00	X
L3 pont on frt axle	L3	80.00	511.00	248.00	X
L6 on rr axle	L6	1,294.00	511.00	255.00	X
L7 point on rr axle	L7	1,434.00	511.00	223.00	X
Wheel Center Rear	W2	1,350.00	919.00	.00	
Rear tire contact point	T2	1,350.00	919.00	-414.00	

Fig. 6 The points and their coordinates. **a** The points defined for front suspension model. **b** The points defined for the rear suspension model

modeled for the first time by using these softwares. The dynamic behavior of the full-vehicle model, which is the representation of the real-life vehicle, is investigated under the simulation scenarios of steady-state cornering and double lane change. Forward velocity, vertical rate of leaf springs causing the roll stiffness of each axle to change, and cornering stiffness of tires are the parameters, effects of which are investigated on the full-vehicle model built. Lateral acceleration, roll angle, yaw rate, vehicle slip angle and axle vertical loads are

a

Component List

Component Name	Used
Front eye bushing	X
Shackle Bushing	X
Weld	X
Kingpin	X
Tie Rod	X
Drag Link	X
Gear	X

b

Component List

Component Name	Used
Bush - LL1	X
Bush - LL2	X
Weld	X
Front spring pivot bushing	X
Beam - Spindle	X
Equalizer Pivot	X
Leaf RH front axle 2 to 1	X
Leaf LH front axle 2 to 1	X
Leaf Slider at Axle	X
Leaf RH front axle 3 to 4	X
Leaf LH Front axle 3 to 4 ...	X
Leaf RH Rear axle 5 to 6	X
Leaf LH Rear axle 5 to 6	X
Leaf RH Rear Axle 7 to 8	X
Leaf LH Rear Axle 7 to 8	X
Constraint - vertical wheel	X

Fig. 7 The components. **a** Components used for front suspension model. **b** Components used for rear suspension model

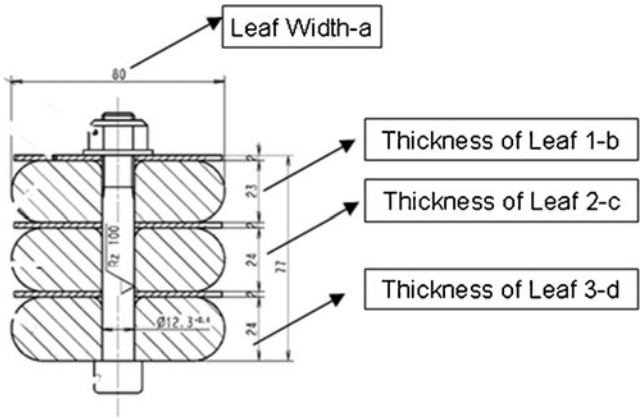

Fig. 8 The cross section of the front leaf spring, nomenclature *a*, *b*, *c*, *d* is given for Eq. 1

the state variables that are calculated through the course of the simulation scenarios.

2 SuspensionSim models

The front suspension consists of front axle, leaf springs, steering system, the stabilizer bar, and the shackles. This type of front suspension is commonly used in this category of commercial vehicles. In Fig. 1, a schematic drawing of the front suspension is given. CATIA 3D model of the front suspension is also given in Fig. 2.

The rear suspension of the tandem rear axles is called "four spring suspension with bar type radius rods" and it consists of leaf springs, the load equalizer, bar-type radius rods, first and second rear axles, and the stabilizer bar. In Fig. 3, a schematic drawing of the rear suspension is given. CATIA 3D model of the rear suspension system is

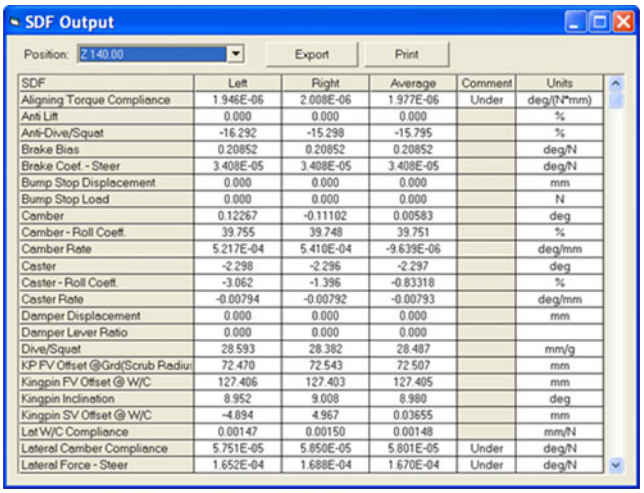
SDF Output

Position: Z 140.00 Export Print

SDF	Left	Right	Average	Comment	Units
Aligning Torque Compliance	1.946E-06	2.008E-06	1.977E-06	Under	deg/(N*mm)
Anti Lift	0.000	0.000	0.000		%
Anti-Dive/Squat	-16.292	-15.298	-15.795		%
Brake Bias	0.20852	0.20852	0.20852		deg/N
Brake Coef. - Steer	3.408E-05	3.408E-05	3.408E-05		deg/N
Bump Stop Displacement	0.000	0.000	0.000		mm
Bump Stop Load	0.000	0.000	0.000		N
Camber	0.12267	-0.11102	0.00583		deg
Camber - Roll Coeff.	39.755	39.748	39.751		%
Camber Rate	5.217E-04	5.410E-04	-9.639E-06		deg/mm
Caster	-2.298	-2.296	-2.297		deg
Caster - Roll Coeff.	-3.062	-1.396	-0.83318		%
Caster Rate	-0.00794	-0.00792	-0.00793		deg/mm
Damper Displacement	0.000	0.000	0.000		mm
Damper Lever Ratio	0.000	0.000	0.000		
Dive/Squat	28.593	28.382	28.487		mm/g
KP FV Offset @Grd(Scrub Radius	72.470	72.543	72.507		mm
Kingpin FV Offset @ W/C	127.406	127.403	127.405		mm
Kingpin Inclination	8.952	9.008	8.980		deg
Kingpin SV Offset @ W/C	-4.894	4.967	0.03655		mm
Lat W/C Compliance	0.00147	0.00150	0.00148		mm/N
Lateral Camber Compliance	5.751E-05	5.850E-05	5.801E-05	Under	deg/N
Lateral Force - Steer	1.652E-04	1.688E-04	1.670E-04	Under	deg/N

Fig. 9 Output of the suspension design factors (SDFs) related to the front suspension model

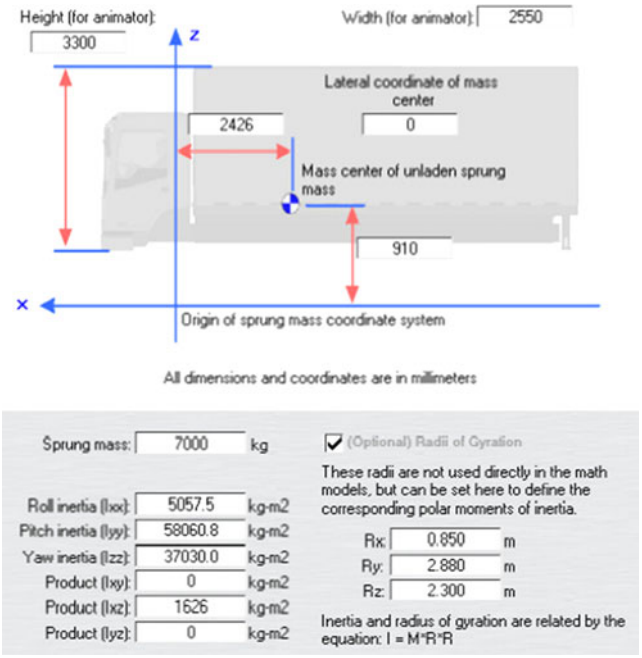

Fig. 10 Dimensions and inertial properties of the vehicle's sprung mass

presented in Fig. 4. All components of the front and rear suspension system that are numbered in Figs. 1 and 3 are presented in Table 1.

The modeling procedure in SuspensionSim is as follows:

- Firstly, the bodies have to be defined. The front and rear suspension models have six and ten bodies, respectively, which are presented in Fig. 5.
- Thereafter, the points are defined. The defined points represent locations of the connections that are essential to assemble the bodies with the components. The points used for the front and rear suspension models are presented in Fig. 6.
- Following, the components, which are presented in Fig. 7, are defined.
- The last step is assembly, i.e., finalizing the construction of the model by establishing the relations between already defined bodies, points, and components.

The leaf springs and stabilizer bars for each suspension model are then integrated to the entire suspension model by using "Leaf Spring" and "Stabar" interfaces. Multi-leaf springs are reduced to their mono-leaf equivalent, which has the same stiffness of the original multi-leaf but comes with a modified thickness called equivalent mono-leaf thickness.

The cross sections of leaf springs are of quasi-perfect rectangular cross section. The cross section of the front leaf spring is presented in Fig. 8. The calculation of the equivalent

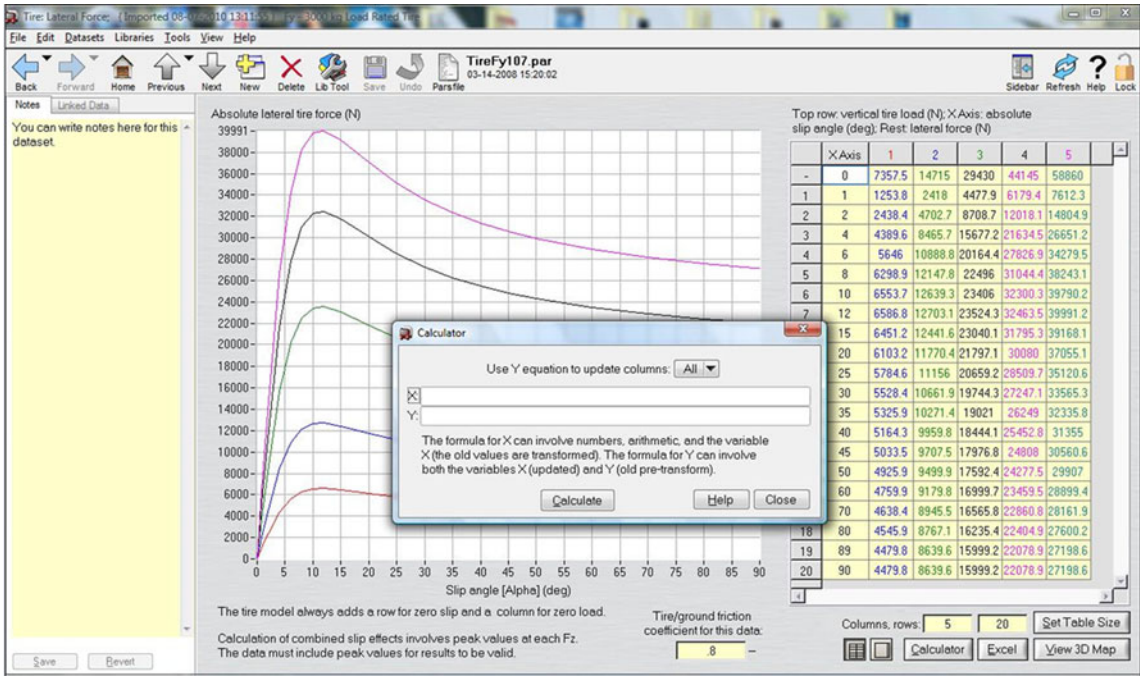

Fig. 11 Defining a new tabular dataset through the use of calculator tool

mono-leaf thickness is given by Eq. 1, where "*I*" is the second moment of area of the rectangular cross sections.

The leaf spring of the front suspension has three leaves, however, on the rear tandem axle; the leaf springs have 15 and 12 leaves, for the first and second rear axle, respectively.

After these steps, the solutions have to be run to acquire suspension design factors (SDFs), i.e., the data containing the kinematics and compliance behavior of the suspension system. The data will be imported to TruckSim. The SDF output of the front suspension solution is presented in Fig. 9.

$$\text{Equivalent thickness} = \sqrt[3]{\frac{12 \times I}{a}}, \quad (1)$$

$$\text{where } I = \frac{1}{12} \times a \times (b^3 + c^3 + d^3)$$

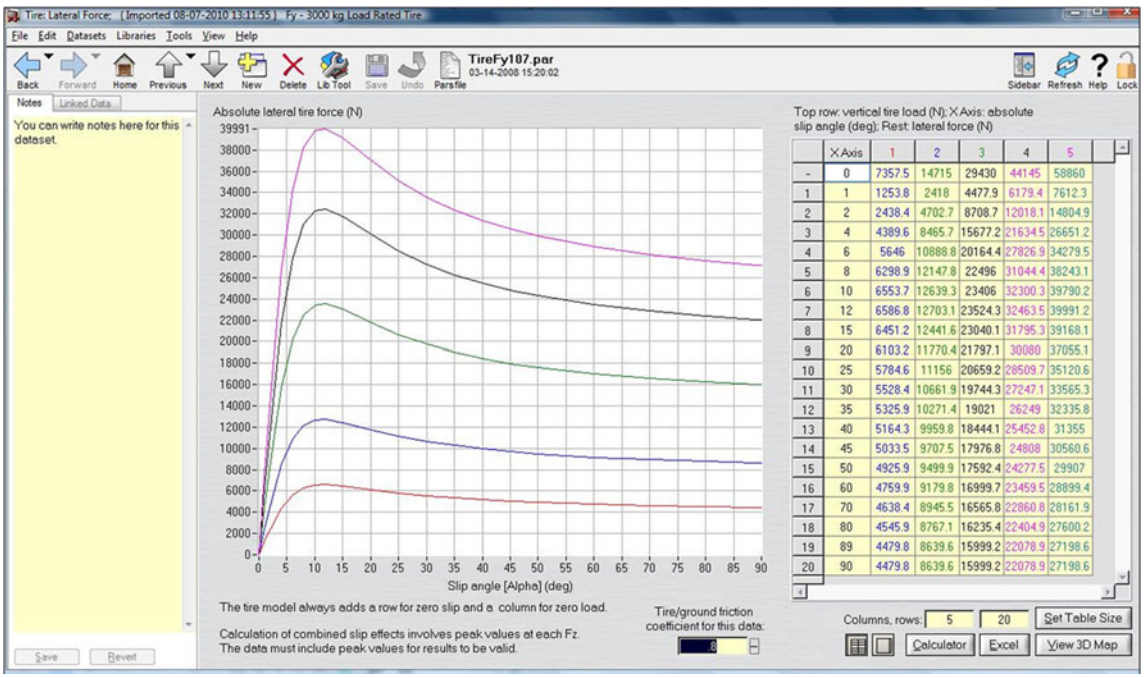

Fig. 12 The relationship between the lateral force on the tire and slip angle for the front tires

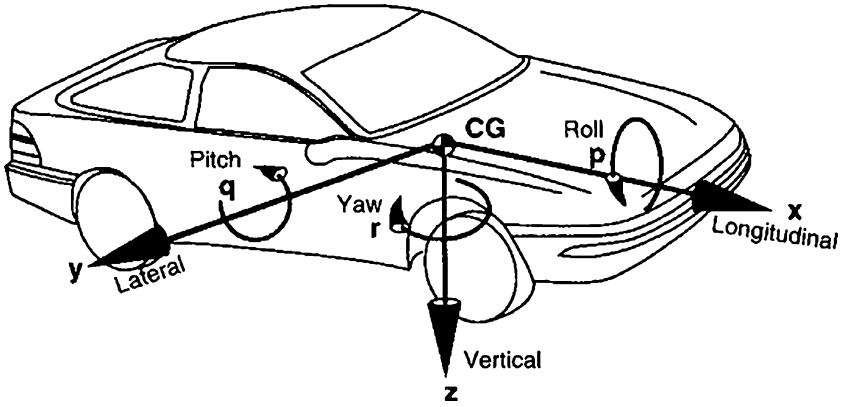

Fig. 13 Vehicle axis system according to SAE convention [8]

3 TruckSim full-vehicle model

The remaining parameters relating to tire, drive train, engine, and brake properties are defined in TruckSim environment. In addition, loading conditions, dimensions, and inertial properties of the vehicle's sprung mass are also defined here. Dimensions and inertial properties of the vehicle's sprung mass are presented in Fig. 10.

Drive train properties are imported to TruckSim from the available gear ratios and shift schedules. It is an 18-speed manual transmission. The air brake patterns available in the library of TruckSim are modified to represent the "brake torque-wheel cylinder pressure" correlation of the real-life vehicle.

An engine, properties of which are tolerably identical to the one used for the real-life vehicle, is selected from the TruckSim library, i.e., the rpm values at which the engine produces maximum power and torque, and its engine map are fairly similar to the real one.

Size of the tires used in actual vehicle is 285/70 R 19.5, and dual tires are used on the first and second rear

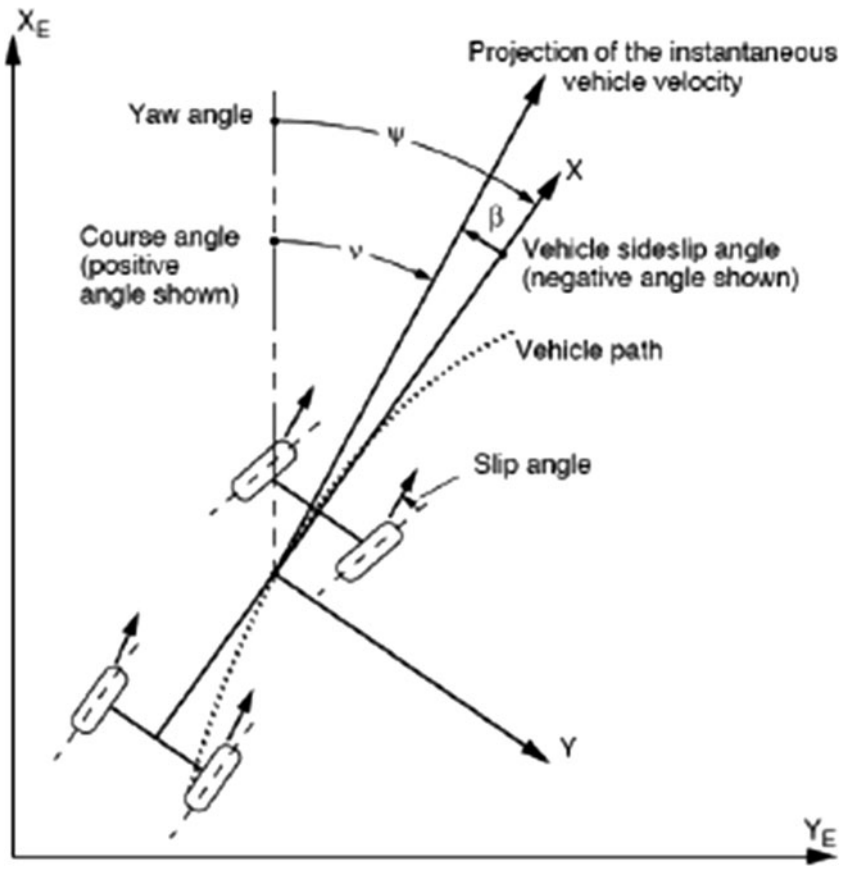

Fig. 14 Earth-fixed axis system defining yaw, vehicle sideslip, course, and slip angles according to SAE convention [9]

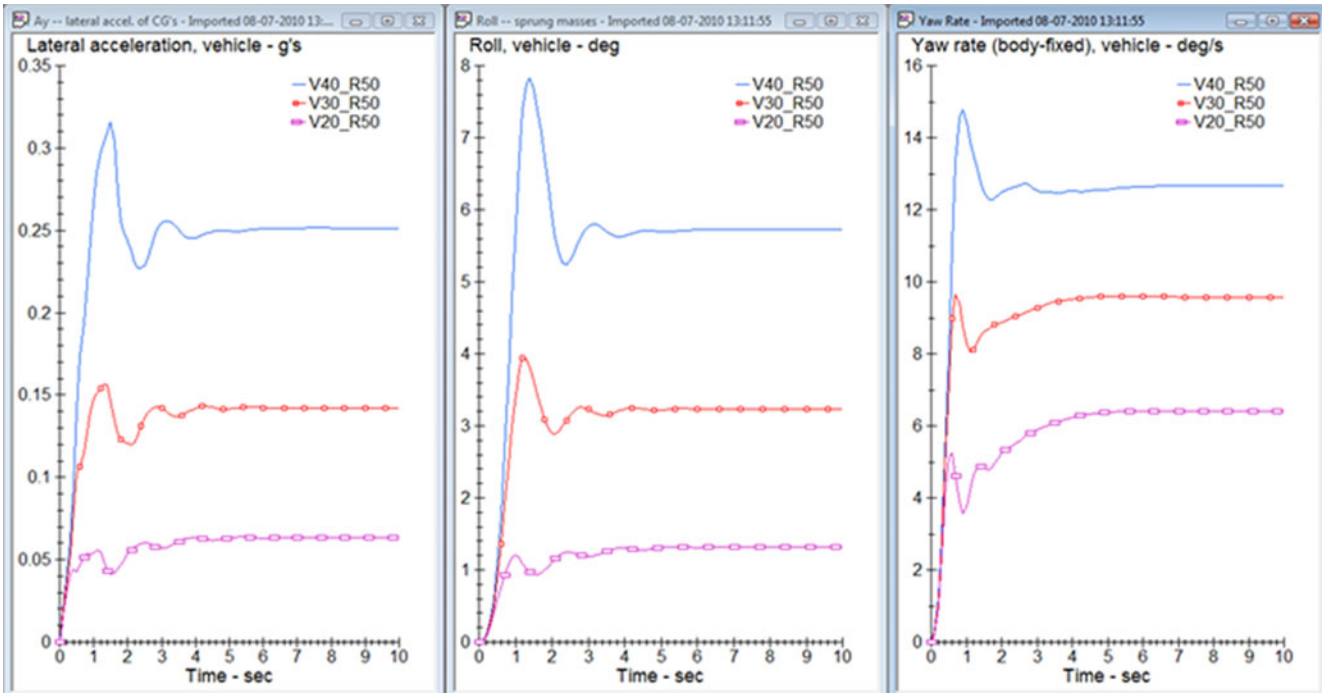

Fig. 15 State variables at various forward velocities and constant radius of curvature; lateral acceleration, roll angle, and yaw rate

axles. Parameters such as effective rolling radius, spring rate, cornering stiffness, camber thrust coefficient, and longitudinal friction coefficient are also provided by the supplier of the tires. All these parameters and physical properties of the tires are entered in the tire interface of the program.

The tire model used is the internal tire model that uses tables with data that define the shear forces and moments, as they would be measured in a laboratory or on-road tester. As is the case in most of the datasets in TruckSim environment provided with tables, the data tables of the tires can be modified by the calculator tool of the TruckSim. For example, a tire dataset already provided for a defined tire force can be modified to define a new tabular dataset relating to a newly defined tire force through the use of calculator tool as it is presented in Fig. 11. The relationship between the lateral force on the tire and slip angle for the front tires is presented in Fig. 12.

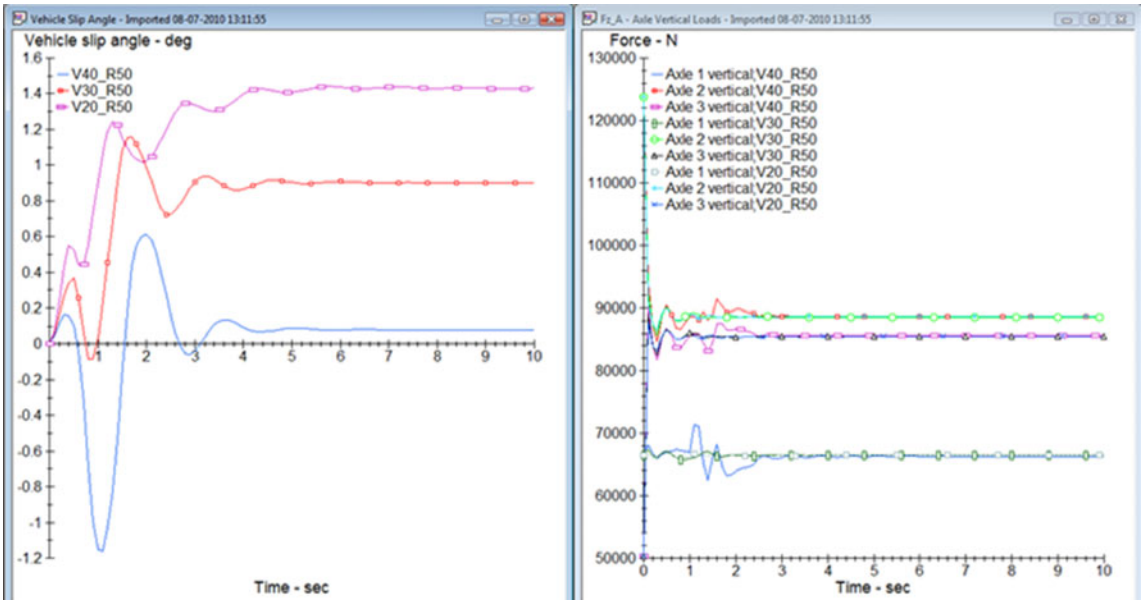

Fig. 16 State variables at various forward velocities and constant radius of curvature; vehicle slip angle and vertical loads

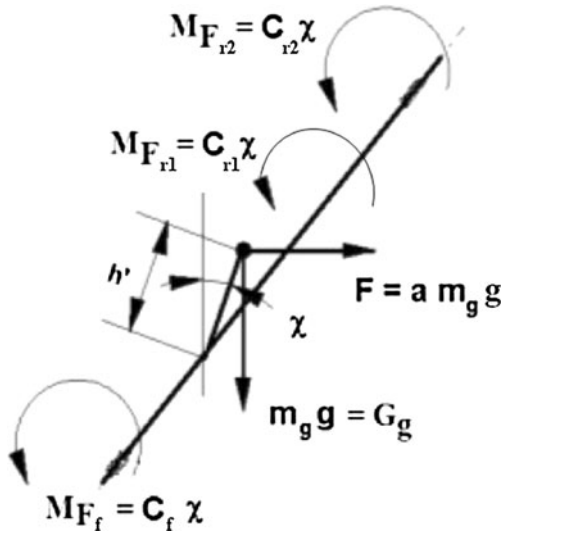

Fig. 17 Forces and moments acting on vehicle's body along its roll axis during steady state cornering. Equilibrium equation of the body, i. e., Eq. 2 is derived accordingly [7]

In the internal tire model, the low-speed behavior of the tire is implemented, as it is in the Pacejka tire model. Pacejka tire model requires many formulations and input parameters such that it requires heavy adjustment work on tire curves. In addition, Pacejka tire model makes it also difficult to modify tire properties of the full-vehicle model [7]. The internal tire model calculates the steady-state behavior of a tire with sufficient accuracy in an effective way.

4 Analyses

Dynamic behavior of the vehicle is examined on two scenarios which are steady-state cornering and double lane change. The conditions related to these scenarios are implemented in TruckSim environment. Vehicle axis system and earth-fixed axis system defining yaw, vehicle sideslip, course, and slip angles according to SAE convention are illustrated in Figs. 13 and 14 [8, 9]. The difference between SAE and ISO convention is that the ISO axis orientation is referred to as the *Z*-up orientation, with the traditional SAE axis orientation referred to as the *Z*-down orientation. These axis orientations

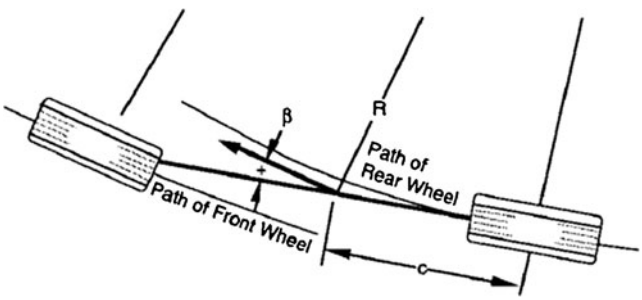

Fig. 18 Vehicle slip angle (or sideslip angle) in a low-speed turn [8]

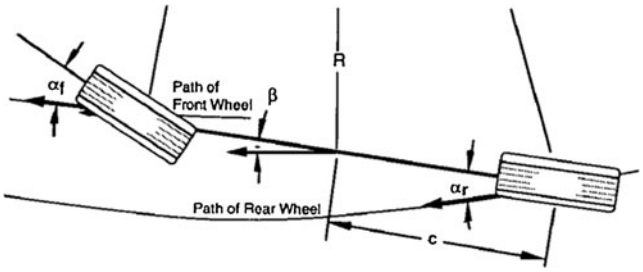

Fig. 19 Vehicle slip angle (or sideslip angle) in a high-speed turn [8]

are equally acceptable, and the selection of the appropriate orientation should be based on the requirements of the analysis or test being performed [9]. In this study, state variables are calculated according to SAE convention.

4.1 Steady-state cornering

State variables—lateral acceleration, roll angle, yaw rate, vehicle slip angle and vertical loads are calculated at various forward velocities of 40, 30, 20 km/h when the vehicle model makes a constant radius turn to the left in steady state. The radius of the curvature of this turn is 50 m. Output plots of the state variables computed are presented in Figs. 15 and 16.

The decrease in the forward velocity, i.e., from 40 to 20 km/h results in the decrease in lateral acceleration, roll angle, and yaw rate but it causes vehicle slip angle to increase. Change in the forward velocity does not cause the vertical loads to change as it can be seen in Fig. 16. Figure 17 [7] represents forces and moments acting on vehicle's body along its roll axis during steady-state cornering. Eq. 2 is the equilibrium equation of vehicle's body.

Theoretically, a reduction in forward velocity causes lateral acceleration and centrifugal force to decrease due to their direct proportionality to velocity. Decrease of the centrifugal force, the second term in Eq. 2, also results in the decrease of roll angle χ.

The real-life vehicle investigated and, thus its model, are presenting understeering behavior. In the case of the understeering vehicle, yaw rate decreases with decreasing forward velocity as it can be seen by the result plot in Fig. 15.

For an understeering vehicle, the opposite scenario, in which forward velocity increases, leads to increase of the yaw rate up to a speed named characteristic speed. Having reached that speed, the yaw rate begins to decrease.

At any point on the vehicle, a sideslip angle or vehicle slip angle may be defined as the angle between the longitudinal axis and the local direction of travel. In general, the sideslip angle will be different at every point on a vehicle during cornering. Taking the center of gravity (CG) as a case in point, the sideslip angle is defined as

Table 2 Exact values of state variables: results of the steady-state cornering simulation

Scenario	Forward velocity V (km/h)	Radius of turn (m)	Lateral acceleration	Roll angle (°)	Yaw rate (°/s)	Vehicle slip angle (°)
1	40	50	0.252	5.72	12.65	0.079
2	30	50	0.142	3.23	9.60	0.902
3	20	50	0.063	1.32	6.41	1.433

shown in Fig. 18. The sideslip angle is defined as positive for this case because the direction of travel (the local velocity vector) is oriented clockwise from the longitudinal axis (clockwise angles viewed from above are positive in SAE convention). At high speed, the slip angle on the rear wheels causes the sideslip angle at the CG to become negative as in Fig. 19 [8].

Under cornering conditions, when forward velocity decreases, tire cornering forces on the tires which the tires must develop to equalize the centrifugal force will decrease. This also leads to the reduction of the slip angle on the rear tires (α_r in Fig. 19).

Any reduction in the slip angle on the rear tires causes the vehicle slip angle or sideslip angle to increase as it can be seen from the result plots in Fig. 16.

The exact numerical values of state variables calculated are given in Table 2.

$$(C_{\mathrm{f}} + C_{\mathrm{r1}} + C_{\mathrm{r2}})\chi - am_g gh' - m_g gh'\chi = 0 \tag{2}$$

where:

C_{f} Roll stiffness of the front axle
C_{r1} Roll stiffness of the first rear axle
C_{r2} Roll stiffness of the second rear axle
χ Roll angle
a Lateral acceleration
m_g Vehicle's mass
g Gravitational acceleration
h' Distance of the center of gravity of vehicle's body from the roll axis

Any change in the vertical rates and lateral separation of leaf springs used for front and rear suspensions affects roll stiffness of axles described in Eq. 2.

The roll stiffness is given by:

$$C = 0.5K_S s^2 \tag{3}$$

where:

C Roll stiffness of axle
K_S Vertical rate of each of the left and right leaf springs
s Lateral separation between the leaf springs

The term C is different for front, first and second rear axles of the vehicle as presented by the terms C_{f}, C_{r1}, C_{r2},

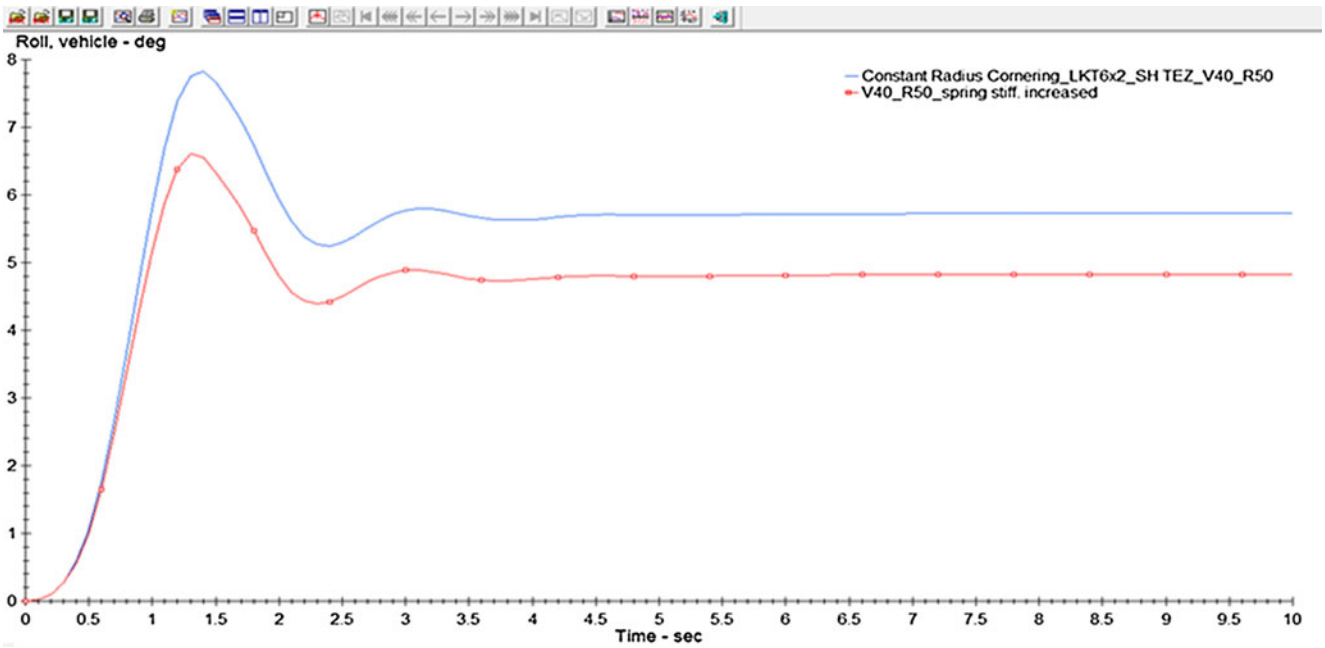

Fig. 20 Results plots of roll angle where *blue plot* represents the modified model and the *red* one the reference model

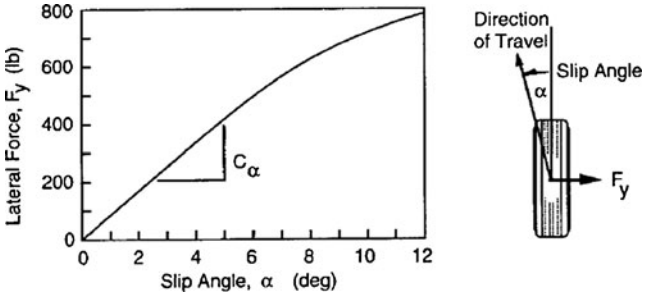

Fig. 21 Tire cornering force properties [8]

in Eq. 2. The roll stiffness of axles develops roll-resisting moments at each axle which is proportional to roll angle χ as presented in Fig. 17.

The roll stiffness of the second axle of the full-vehicle model is increased by increasing the vertical rate of the leaf springs at that axle, and accordingly, a simulation run is made where the full-vehicle model turns a radius of curvature of 50 m at a constant forward velocity of 40 km/h as in scenario 1 in Table 2. Such a change will have a remarkable effect on the roll angle χ while not affecting any other state variables described previously. Figure 20 compares the roll angles of the modified model and the reference model, i.e., no change in roll stiffness. The modified full-vehicle model turns the radius with a roll angle of 4.81°, whereas the reference model turns with a roll angle of 5.72° as it is provided for scenario 1 in Table 2.

A theoretical explanation for the decrease in roll angle will come from Eqs. 2 and 3. According to Eq. 3, an increase in K_s of the leaf spring at the second rear axle will result in the increase in C_{r2} term described by Eq. 2. Therefore, the roll angle χ of the modified model will be smaller than that of the reference model.

Cornering stiffness C_α of a tire is defined as the slope of the curve for tire cornering force F_y versus slip angle α at $\alpha=0$ which is illustrated in Fig. 21 [8]. At low slip angles (5° or less) the relationship between them is described as in Eq. 4. Cornering stiffness of a tire is dependent on variables such as tire size and type (radial versus bias-ply construction), number of plies, cord angles, wheel width, and tread for a given vertical load and inflation pressure.

$$F_y = C_\alpha \alpha \tag{4}$$

The cornering stiffness of tires of the full-vehicle model representing the real-life vehicle is denoted by C_2. The cornering stiffness of tires of the full-vehicle model is changed such that $C_3 > C_2 > C_1$ and a simulation run is made in which these three models make a constant radius cornering with a radius of curvature of 50 m, at a constant forward velocity of 40 km/h. This modification has an important effect on vehicle slip angle while any changes in other state variables described previously are not noteworthy. The plots of vehicle slip angle are provided in Fig. 22.

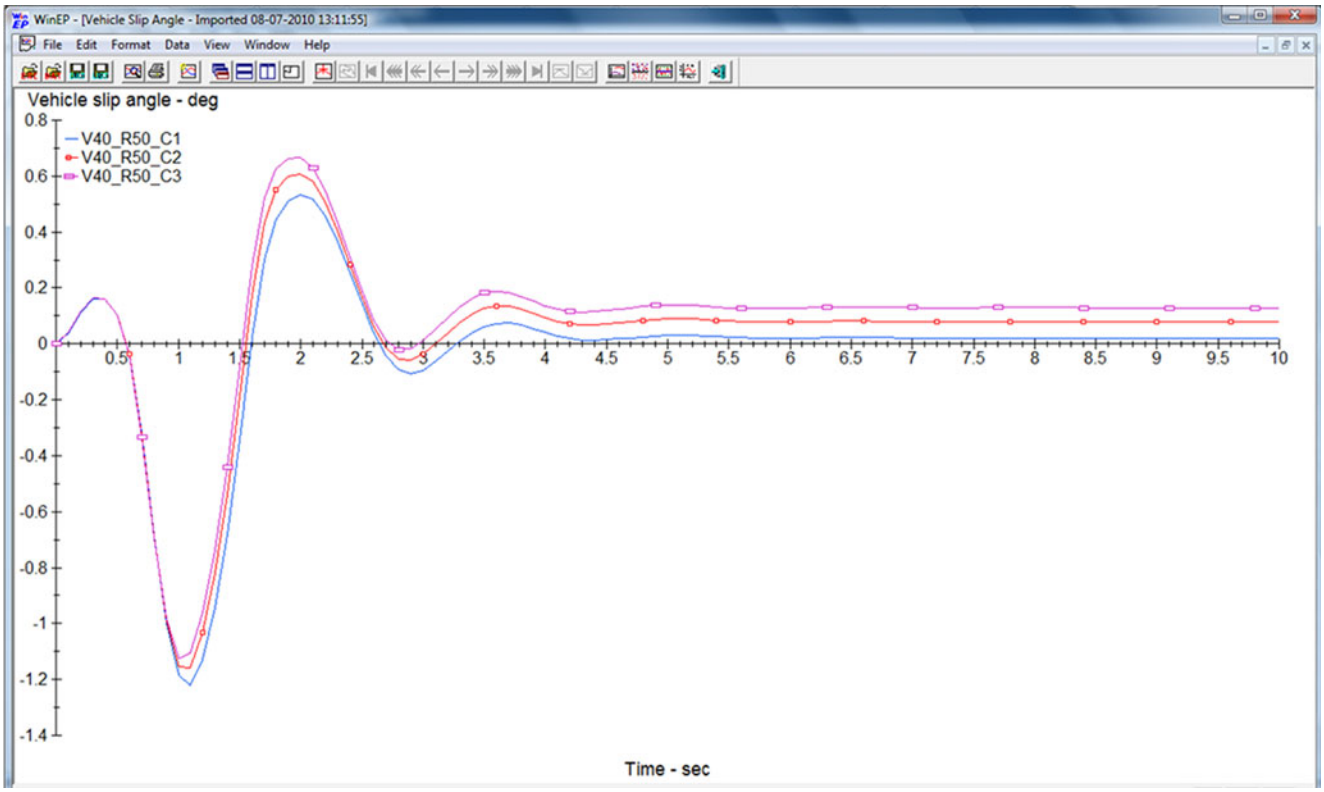

Fig. 22 Change in vehicle slip angle due to the change in tire cornering stiffness

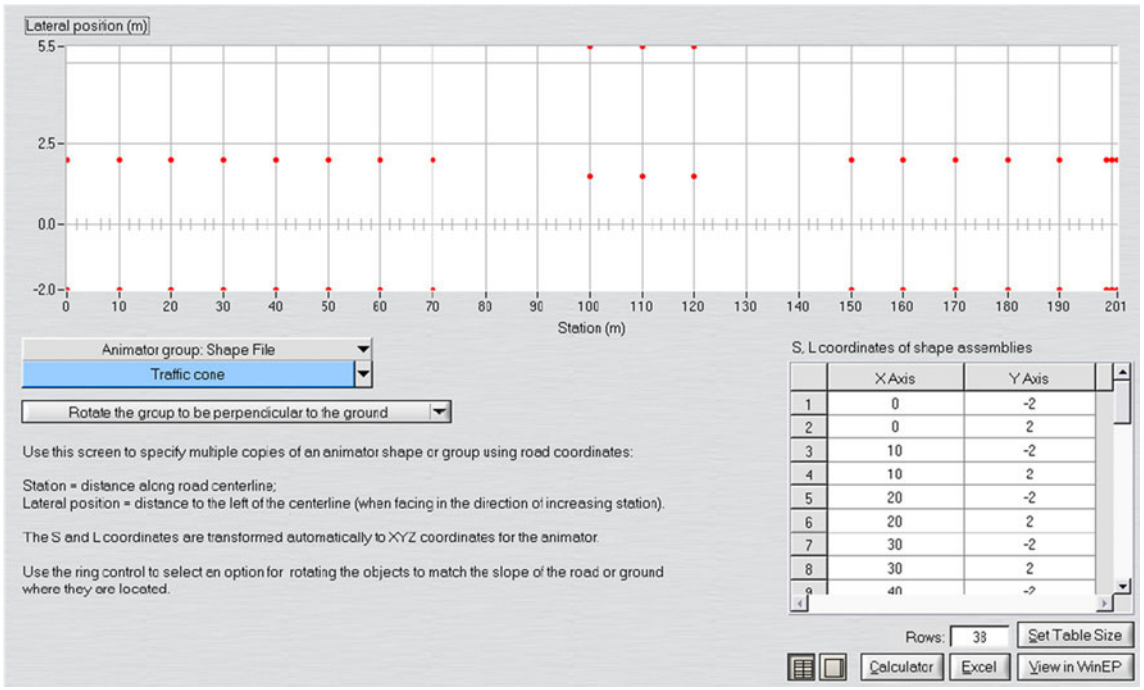

Fig. 23 Road profile for double lane change scenario

As it can be noted in Fig. 22, a higher cornering stiffness results in a higher vehicle slip or sideslip angle. Cornering forces on each tire equalizing the centrifugal force are the same for each vehicle model.

Hence, according to Eq. 4, the slip angles will be lower for tires having a higher cornering stiffness. As it is mentioned before, a lower slip angle, especially in rear tires, will cause the vehicle slip angle to increase.

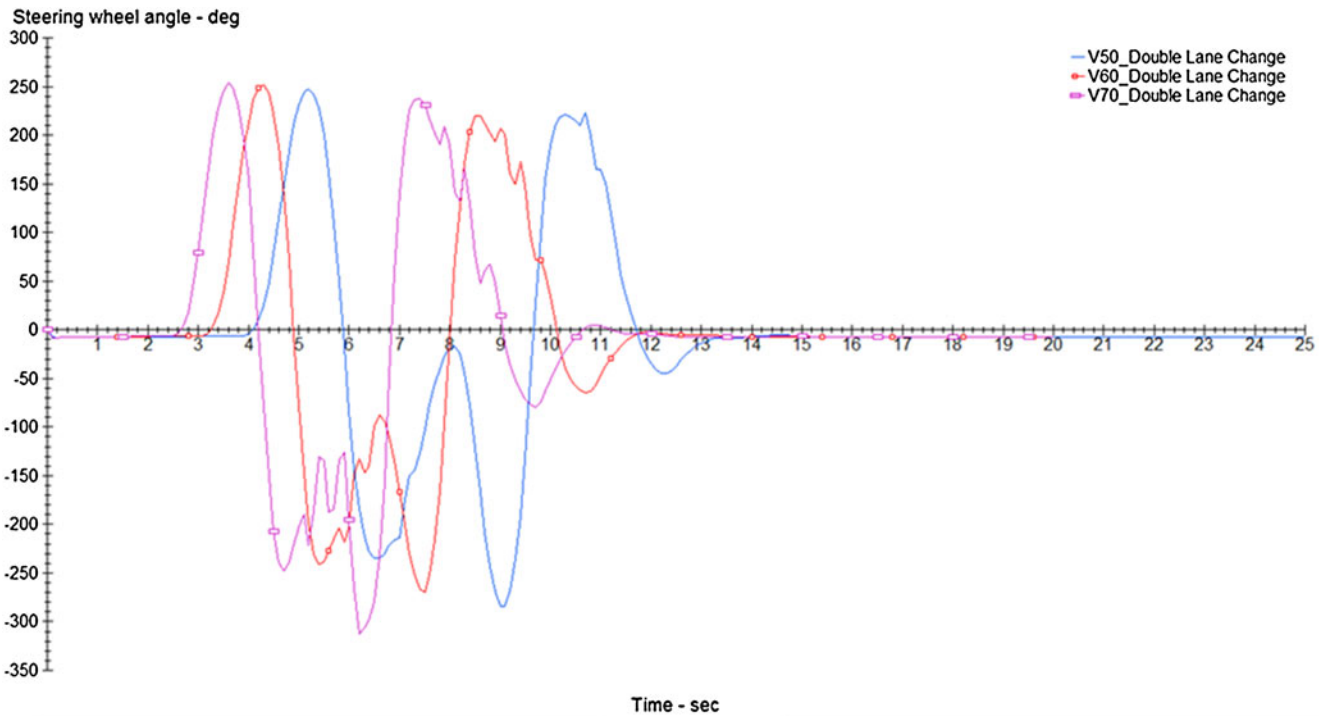

Fig. 24 The changes in state variables at different forward velocities: steering wheel angle

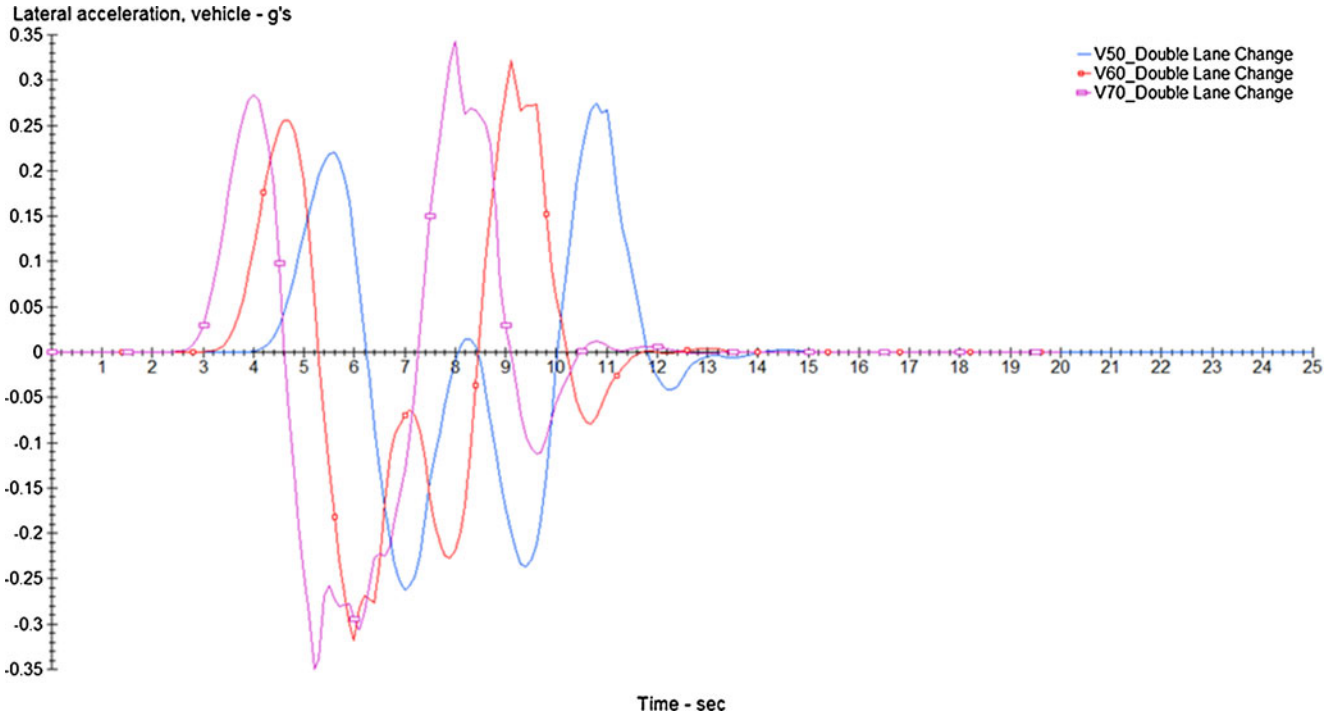

Fig. 25 The changes in state variables at different forward velocities: lateral acceleration

4.2 Double lane change

Dynamic behavior of the full-vehicle model is also investigated through a double lane change simulation scenario. The road profile is provided in Fig. 23.

The vehicle starts moving at zero station and lateral position point, moves through the traffic cones, makes first lane change to the left with respect to the direction of motion, makes second lane change to the right, and moves straight ahead thereafter without any change in steering wheel angle. Driver controls

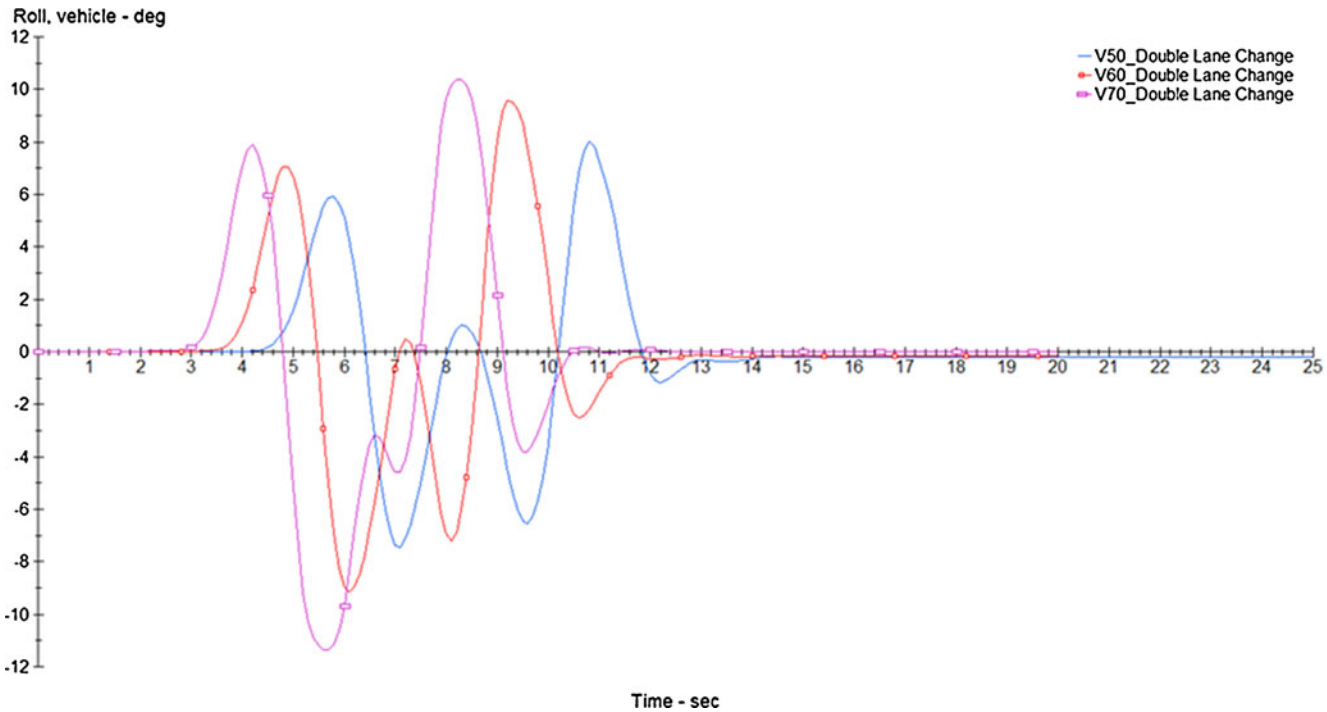

Fig. 26 The changes in state variables at different forward velocities: roll angle

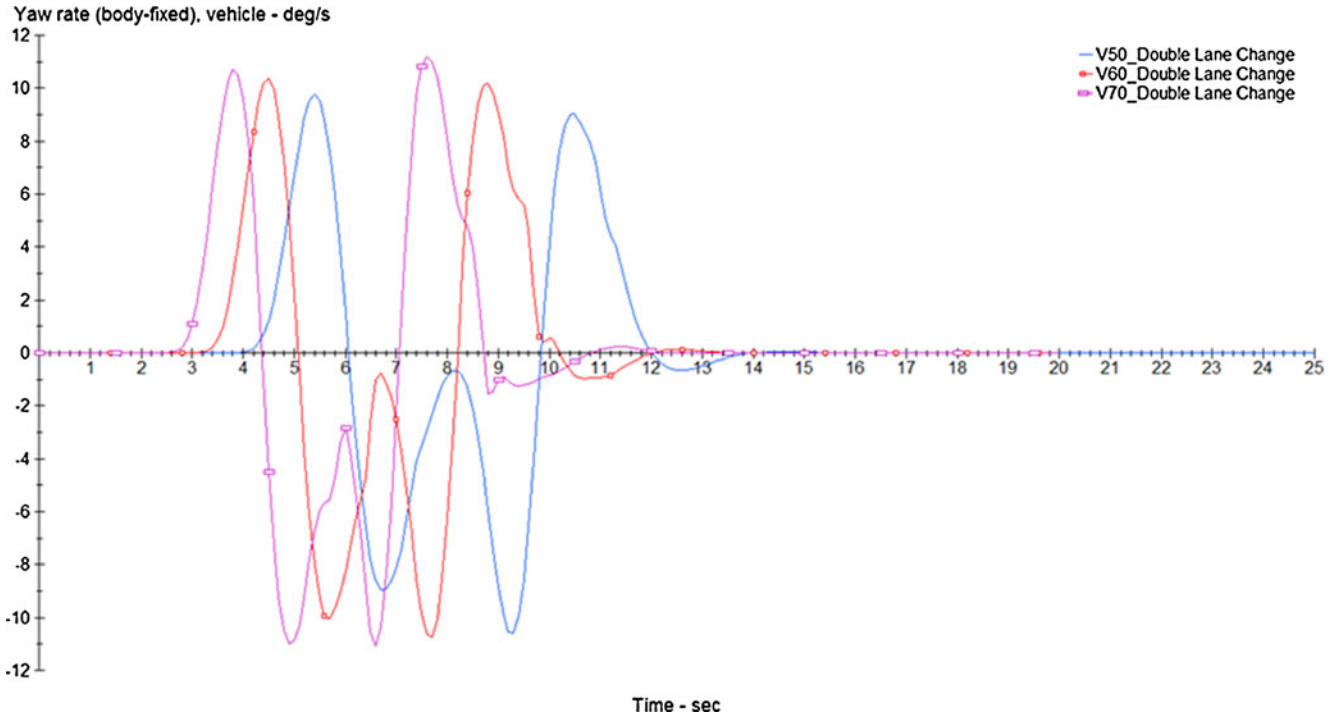

Fig. 27 The changes in state variables at different forward velocities: yaw rate

used by TruckSim are also worth mentioning here. TruckSim provides both closed-loop and open-loop driver controls. Driver control used for this study is named as steering by the driver model that operates with a closed-loop controller to follow a target path at a target speed. Simulation runs are made at forward velocities of 50, 60, and 70 km/h, respectively.

The changes in state variables during the course of double lane change maneuver are presented by plots in

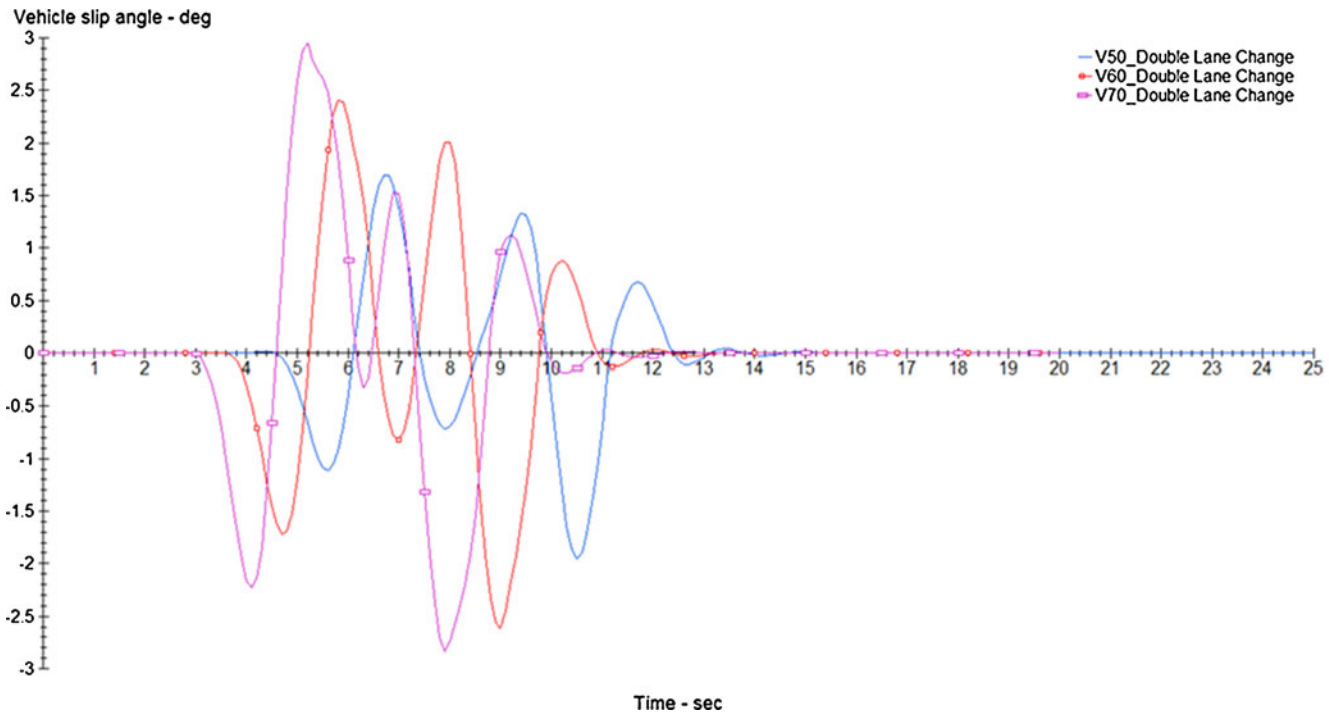

Fig. 28 The changes in state variables at different forward velocities: vehicle slip angle

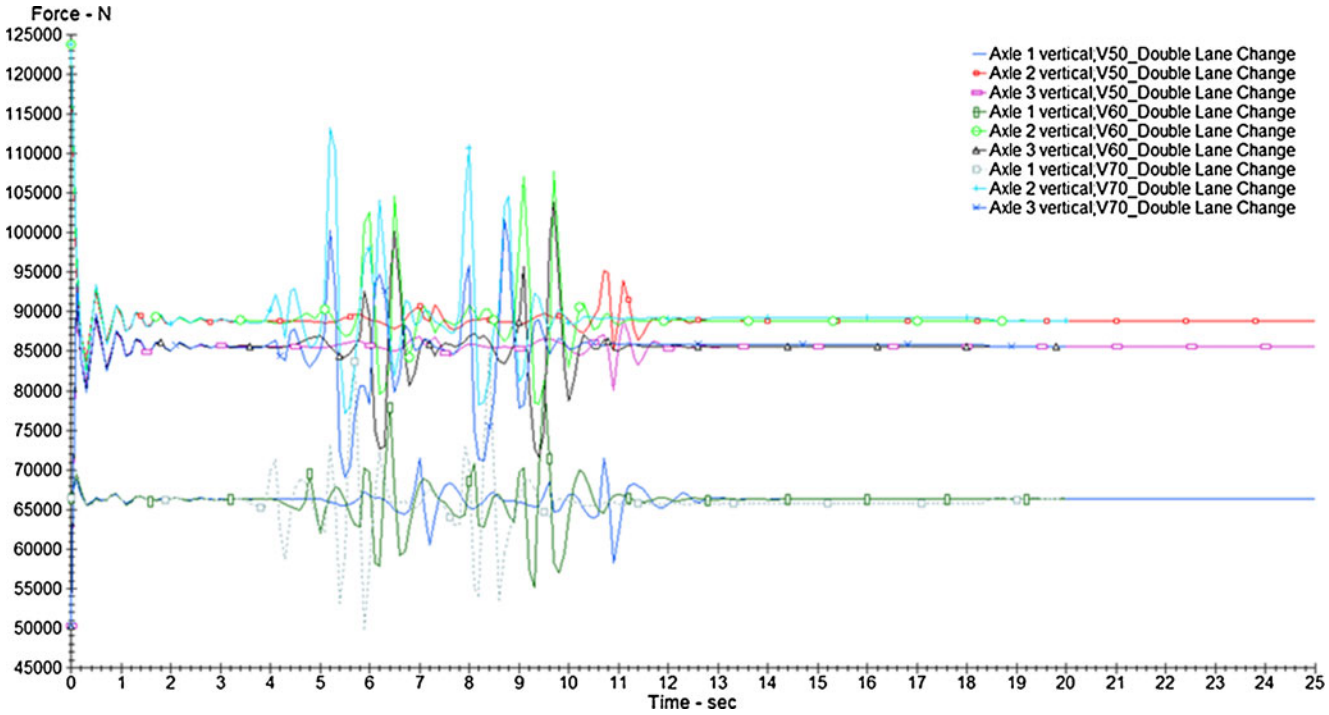

Fig. 29 The changes in state variables at different forward velocities: vertical load at each axle

Figs. 24, 25, 26, 27, 28, and 29. Minimum and maximum values of state variables plotted are given in Table 3.

Steering wheel angle changes presented in Fig. 24 are explanatory to ascertain the changes of direction of the vehicle during the maneuver. The first peak indicating a positive steering wheel angle value represents the first lane change to the left. Thereafter, there are steering wheel corrections, and then the second lane change to the right followed by subsequent steering wheel corrections takes place. As it can be seen in Figs. 25, 26, and 27, the peak values of lateral acceleration, roll angle, and yaw rate are decreasing as forward velocity is decreasing. Moreover, absolute peak values of vehicle slip angle, which are represented in Fig. 28, are smaller at lower forward velocities. As forward velocity increases, there are bigger oscillations of vertical load at each axle in the time interval in which the vertical load at each axle is in dynamic character (Fig. 29). In addition, the difference between minimum and maximum values of the vertical load at each axle is increasing as forward velocity is increasing as indicated in Table 3.

5 Concluding remarks

Increase in vehicle complexity and competition in the market result in reduction of time available for the product development. A cheaper and less time-consuming alternative is using simulations of mathematical models of the proposed vehicles.

Table 3 Minimum and maximum values of state variables upon double lane change simulation results

	At 50 km/h		At 60 km/h		At 70 km/h	
State variables	min	max	min	max	min	max
Steering wheel angle (°)	−284.003	247.575	−269.819	251.368	−312.410	253.664
Lat. acc.	−0.262	0.273	−0.318	0.322	−0.350	0.342
Roll angle (°)	−7.439	8.012	−9.177	9.577	−11.354	10.381
Yaw rate (°/s)	−10.591	9.767	−10.726	10.382	−11.087	11.191
Vehicle slip angle (°)	−1.957	1.696	−2.615	2.403	−2.833	2.949
1. axle vertical load (N)	58,288.63	71,507.01	55,125.86	81,312.26	49,891.70	84,712.21
2. axle vertical load (N)	83,682.59	123,801.92	78,360.79	123,812.41	77,222.90	123,828.32
3. axle vertical load (N)	50,274.68	91,322.93	50,262.43	103,724.02	50,225.11	103,746.41

The objective of this paper is to build the full-vehicle model of a commercial vehicle and examine its dynamic behavior by using MBS methods becoming important steps of virtual prototyping adapted in the automotive industry. The models related to the front and rear suspensions were prepared in SuspensionSim software and the solutions were imported thereafter to TruckSim.

Full-vehicle model excluding suspension system is formed by using TruckSim software. The simulation scenarios whose runs were made to observe the effects of different parameters on the dynamic behavior of the full-vehicle model are also prepared in TruckSim environment. The proposed full-vehicle model will be also used for modeling other real-life vehicles having similar configuration regarding the suspension system and other vehicle subsystems. The rear suspension model is built for the first time by using SuspensionSim and TruckSim MBS softwares.

Models generated not only underlay both basis and patterns of the similar suspension and vehicle configurations but also help to execute visually perfect, safe, and repeatable test procedures which results in reduction of time and money consumed. The necessity to solve theoretical relations between vehicle subsystems together also provides an opportunity to identify some vehicle parameters that are likely to optimize. The results obtained will also be useful while performing tests for validation of the full-vehicle model.

This study is also beneficial in a sense of taking an active hand to develop the softwares with the collaboration of its producers which involves not only the versions up to date but also future versions of the softwares. Some additional features like modeling air springs and new truck suspension types, and adding additional axles will be ensured by the next version of the programs which is also a substantial step considering implementing and developing simulation techniques that are more real than their predecessors.

Acknowledgments The authors would like to thank to Dr. Thomas Gillespie, co-founder of "Mechanical Simulation Company"; Joe Knable, founder of Knable & Associates, Inc.; and Dr. Cengiz Bozkurt, vehicle dynamics specialist at Daimler AG.

References

1. Sayers MW (1999) Vehicle models for RTS applications. Veh Syst Dyn 32:421–438
2. Mechanical Simulation Corporation (MSC) (2009) TruckSim v8.0 Technical Memos, Reference Manuals & Release Notes
3. Gillespie T (2005) Using vehicle dynamics simulation as a teaching tool in automotive engineering courses, SAE Technical Paper Series, 2005
4. Riedel A, Schmidt A (2001) Testing control systems of trucks and truck–trailer-combinations with hardware in the loop-very real tests in a virtual world, SAE Technical Paper Series, 2001-01-2768
5. Chandrasekharan S, Guenther D, Heydinger G, Salaani K, Zagorski S, Grygier P (2010) Simulation results from a model of a tractor trailer vehicle equipped with roll stability control, SAE International, 2010-01-0098
6. Hegazy S, Sandu C (2010) Evaluation of heavy truck ride comfort and stability, SAE International, 2010-01-1140
7. Hasagasioglu S (2010) Vehicle dynamics analysis of a 6×2 heavy duty commercial vehicle by using numerical methods, Master's Thesis, ITU Institute of Science and Technology
8. Gillespie T (1992) Fundamentals of vehicle dynamics, SAE International, 1992
9. SAE Publications (2008) Vehicle dynamics terminology, SAE International, No. J670